

## Hydrogenic impurities in triangular GaAs quantum wells

J. M. Ferreyra\* and C. R. Proetto

*Centro Atómico Bariloche, 8400 San Carlos de Bariloche, Rio Negro, Argentina*

(Received 2 October 1990; revised manuscript received 22 February 1991)

A variational calculation of the ground state of shallow donors and acceptors in triangular GaAs quantum wells is presented. This is connected to the properties of hydrogenic impurities in sawtooth-doped (or  $\delta$ -doped  $n$ - $i$ - $p$ - $i$ ) superlattices. The binding energy, lateral extension, and vertical extension are calculated as functions of the impurity position in the well and  $\delta$ -doping concentration.

### I. INTRODUCTION

Steady improvements in methods of epitaxial growth,<sup>1</sup> such as molecular-beam epitaxy (MBE) and metal-organic chemical vapor deposition (MOCVD) during the past decade, have provided the capability of producing high-quality semiconductor heterostructures having designed potential profiles and impurity distributions with a dimensional control close to interatomic spacing and with virtually defect-free interfaces. These semiconductor heterostructures have given rise to a rich set of new physics as well as devices.<sup>2</sup>

These systems can be classified into two classes: compositional and doping superlattices.

In the case of the now familiar compositional superlattices, the band-edge modulation that gives rise to the periodic potential has its origin in the different band gaps of the components: the archetypical example is GaAs-Ga<sub>1-x</sub>Al<sub>x</sub>As. These types of superlattices allow an unambiguous observation of intrinsic features such as quantum-confined interband transitions<sup>3</sup> and extrinsic features related to the presence of donor<sup>4-6</sup> and acceptor<sup>7</sup> impurities in the quantum wells. A detailed list of theoretical and experimental work on hydrogenic impurities in GaAs-Ga<sub>1-x</sub>Al<sub>x</sub>As quantum wells can be found in recent reviews on the subject.<sup>8-12</sup>

On the other hand, only very recently has it been possible to observe clearly size quantization in doping superlattices.<sup>13-16</sup> Doping superlattices consist of alternating  $n$ -type and  $p$ -type doped layers separated by intrinsic regions of an epitaxially grown semiconductor (for a review on early work see Ref. 17). A sawtooth-shaped band diagram is obtained if the thickness of the doped layer decreases, such that the dopants are localized on a scale length of a lattice constant.

Besides size quantization, very recently excitonic effects in sawtooth-doping superlattices have also been studied experimentally<sup>13</sup> and theoretically.<sup>18</sup>

It is the purpose of this work to report on our variational calculations of hydrogenic donor and acceptor impurities in triangular GaAs quantum wells. In the limit of weak coupling between adjacent quantum wells, this is connected to the properties of shallow impurities in sawtooth-doped superlattices. We have studied the binding energy, lateral and vertical extension of the impurity

as function of its position in the well, and  $\delta$ -doping concentration.

It should be pointed out that in a very early proposal on the interesting properties of  $\delta$ -doped  $n$ - $i$ - $p$ - $i$  structures by Döhler,<sup>19</sup> he estimates the change of energy for on-center hydrogenic impurities in triangular potentials.

The rest of the paper is organized as follows. In Sec. II we describe in detail our model Hamiltonian, the variational wave function we use to solve it, and the corresponding expressions for the expectation values of the different physical magnitudes (binding energy, lateral and vertical extensions). In Sec. III, we give the numerical solution of these expectation values and discuss our results.

### II. THEORY

We assume that adjacent wells corresponding to the same band are sufficiently isolated by thick barriers so as to be independent (the quantum-well regime). We have recently calculated the band structure and charge distribution of sawtooth-doped superlattices<sup>20</sup> as a function of period and doping concentration. For a given level of doping, it is always possible to find a period where the superlattice is in the quantum-well regime. For example, for a typical impurity concentration of  $1.25 \times 10^{13}/\text{cm}^2$ , the superlattice can be considered as a set of independent quantum wells (at least with regard to the first electron and hole subbands) for a period of 150 Å.<sup>20</sup>

In accordance with that simplifying assumption, the shallow impurity state is composed of a hydrogenic atom squeezed in a triangular potential well. In the case of the acceptors, we neglect the coupling of the top four valence bands, and consider a spherical hole effective mass.

Within the effective-mass approximation, the Hamiltonian of a hydrogenic impurity in a triangular quantum well is given by

$$H = H_0 + H_1 \quad (1)$$

with

$$H_0 = -\frac{\hbar^2}{2m^*} \frac{\partial^2}{\partial z^2} + eF|z| \quad (2)$$

and

$$H_1 = -\frac{\hbar^2}{2m^*} \frac{1}{\rho} \frac{\partial}{\partial \rho} \left[ \rho \frac{\partial}{\partial \rho} \right] - \frac{e^2}{\epsilon[\rho^2 + (z - z_i)^2]^{1/2}}. \quad (3)$$

The particle position is represented by cylindrical coordinates  $\rho$  and  $z$  (we have chosen the origin of coordinates at the vertex of the V-shaped well and the polar axis along the growth direction).  $z_i$  is the coordinate of the impurity site along the superlattice axis.

The built-in electric field  $F$  is related to the  $\delta$ -doping concentration  $N^{2D}$  according to the equation

$$F = \frac{2\pi e N^{2D}}{\epsilon}. \quad (4)$$

The carrier effective mass and the GaAs dielectric constant are represented by  $m^*$  ( $m_e^*$  for electrons,  $m_h^*$  for holes) and  $\epsilon$ , respectively.

Before we embark on the solution of the quantum-mechanical problem represented by Eqs. (1)–(3) we will discuss briefly the simplifying assumption made in our treatment of the spatial charge of the impurities as a continuous charge distribution (“jellium” model). That approximation implies that we are neglecting the spatial potential fluctuations which result from the random distribution of impurities in the doped planes.

This is a complicated problem that has been discussed in some detail in the past.<sup>21–23</sup> Without going into a detailed analysis of this point, we want at least to justify its plausibility as a consequence of the following.

(i) The potential fluctuations will be partially screened by a small concentration of free electrons in the  $n$ -type planes (holes in the  $p$ -type planes). The presence of free carriers is impossible to be avoided, as experimentally the condition of exact compensation ( $N_A^{2D} = N_D^{2D}$ ) is fulfilled with a tolerance of about 10%.<sup>24</sup>

(ii) The potential fluctuations are minimized in the case of a doping profile consisting of a train of  $\delta$  functions, as compared with other doping profiles.<sup>22,23</sup> This is related

with the fact that in the case of a  $\delta$  doping, one is suppressing the fluctuations related to random distributions of impurities in the superlattice (growth) direction.

It is interesting to point out that the same model applies without modifications to the problem of shallow impurity states in compositionally graded superlattices,<sup>25</sup> where a quasi-electric-field  $F$  is obtained by a gradual change of the alloy composition of ternary alloy semiconductors. These superlattices are clearly free from the above-mentioned approximations related to the treatment of the impurity charges.

As an exact solution of the problem posed by Eqs. (1)–(3) is not available, we propose the following variational wave function:

$$\psi(\mathbf{r}) = N f(z) e^{-\sqrt{\gamma^2 \rho^2 + \eta^2 (z - z_i)^2}}, \quad (5)$$

where  $\gamma$  and  $\eta$  are variational parameters and  $f(z)$  is the exact solution of  $H_0$  given by

$$f(z) = \begin{cases} \text{Ai}[-(\alpha - z)\beta], & z > 0 \\ \text{Ai}[-(\alpha + z)\beta], & z < 0 \end{cases} \quad (6)$$

with  $\alpha = E_0/eF$ , and  $\beta = (2m^*eF/\hbar^2)^{1/3}$ . Here  $\text{Ai}(z)$  is the Airy function,<sup>26</sup> and  $E_0$  is the energy of the first electron or hole subband.

For a given value of the electric field  $F$  [or equivalently of  $N^{2D}$ , according to Eq. (4)],  $E_0$  and  $F$  are related by the equation<sup>13</sup>

$$E_0 = |a'_1| \left[ \frac{\hbar^2 e^2 F^2}{2m^*} \right]^{1/3}, \quad (7)$$

where  $|a'_1| = 1.02$  is the first zero of the derivative of the Airy function.<sup>26</sup>

Finally  $N$  is a normalization constant, defined by the relation

$$N = \left[ \frac{\pi}{2\gamma^2} \int_{-\infty}^{\infty} dz f^2(z) e^{-2\eta|z - z_i|} (1 + 2\eta|z - z_i|) \right]^{-1/2}.$$

Once  $E_0$  and  $f(z)$  are determined for a given value of  $N^{2D}$ , the mean value of the energy is obtained according to

$$E(\eta, \gamma) = \frac{\langle \psi | H | \psi \rangle}{\langle \psi | \psi \rangle} \quad (8a)$$

$$= E_0 + \frac{\hbar^2}{2m^*} (\eta^2 + \gamma^2) - 2\pi N^2 \int_{-\infty}^{\infty} dz f^2(z) \int_0^{\infty} d\rho \rho \left[ \frac{\hbar^2}{2m^*} \eta^2 \gamma^2 \left[ \frac{\rho^2 + (z - z_i)^2}{\gamma^2 \rho^2 + \eta^2 (z - z_i)^2} \right] + \frac{e^2}{\epsilon[\rho^2 + (z - z_i)^2]^{1/2}} \right] e^{-2[\gamma^2 \rho^2 + \eta^2 (z - z_i)^2]^{1/2}}. \quad (8b)$$

Minimization of (8b) with respect to  $\eta$  and  $\gamma$  gives the minimum value  $E_{\min}$ , so we define the impurity binding energy as

$$E(N^{2D}, z_i) \equiv -E_{\min} + E_0. \quad (9)$$

In addition to the binding energy, the expectation values  $\langle \rho \rangle$  and  $\langle (z - z_i)^2 \rangle^{1/2}$  are relevant quantities which are useful to ascertain the accuracy of a trial wave function, as they provide some insight into its spatial ex-

tension. It should be pointed out that our trial wave function is an exact solution of the Hamiltonian (1) in both limits  $N^{2D} \rightarrow 0$  and  $N^{2D} \rightarrow \infty$ .

For  $N^{2D} \rightarrow 0$  and  $z_i = 0$ ,  $f(z) \rightarrow \text{const}$ ,  $\gamma \rightarrow \eta \rightarrow 1/a_0^*$ , and Eq. (5) reduces to the ground state of the three-dimensional hydrogen atom

$$\psi(\mathbf{r}) \rightarrow \frac{1}{(\pi a_0^{*3})^{1/2}} e^{-(\rho^2 + z^2)^{1/2}/a_0^*} \quad (10)$$

with  $a_0^*$  (the effective Bohr radius)  $= \epsilon \hbar^2 / m^* e^2$ . Also the expectation values of the different magnitudes approach asymptotically the corresponding 3D limits:

$$E(N^{2D} \rightarrow 0, 0) \rightarrow 1 \text{ Ry}^* = \frac{m^* e^4}{2\epsilon^2 \hbar^2}, \quad (11)$$

$$\langle \rho \rangle \rightarrow \frac{3}{8} \pi a_0^*, \quad (12)$$

$$\sqrt{\langle z^2 \rangle} \rightarrow a_0^*. \quad (13)$$

For  $N^{2D} \rightarrow \infty$  and  $z_i = 0$ ,  $f(z) \rightarrow \delta(z)$ ,  $\gamma \rightarrow a_0^*/2$ ,  $\eta \rightarrow 0$ , and expression (5) reduces to the ground state of a two-dimensional hydrogen atom

$$\psi(\mathbf{r}) \rightarrow \left[ \frac{8}{\pi a_0^{*2}} \right]^{1/2} e^{-2\rho/a_0^*} \quad (14)$$

with corresponding values of the expectation values

$$E(N^{2D} \rightarrow \infty, 0) \rightarrow 4 \text{ Ry}^*, \quad (15)$$

$$\langle \rho \rangle \rightarrow a_0^*/2, \quad (16)$$

$$\langle z^2 \rangle^{1/2} \rightarrow 0. \quad (17)$$

The values of the physical parameters we use in the calculations are  $m_e = 0.0667m_0$ ,  $m_h = 0.30m_0$  (Ref. 27) ( $m_0$  is the free-electron mass), and  $\epsilon = 12.5$ . The equivalent three-dimensional effective Rydberg energy ( $\text{Ry}^*$ ) and Bohr radius ( $a_0^*$ ) with these parameters are 6 meV (26 eV) and 100 Å (22 Å) for donors (acceptors). The corresponding two-dimensional effective Rydberg energy (4  $\text{Ry}^*$ ) and Bohr radius ( $a_0^*/2$ ) are 24 meV (104 meV) and 50 Å (11 Å) for donors (acceptors).

### III. RESULTS AND DISCUSSION

In Fig. 1 the on-center ( $z_i = 0$ ) donor (left scale) and acceptor (right scale) binding energies are plotted as functions of  $N^{2D}$ .

For small values of  $N^{2D}$ , the triangular potential is very shallow, and both the donor and the acceptor binding energies approach asymptotically their respective 3D limits. For  $N^{2D} = 10^{10}/\text{cm}^2$  it is hard to distinguish any confinement effect.

For larger values of  $N^{2D}$ , the triangular potential becomes deeper, with a consequent increase of the binding energies, towards the maximum value of 4  $\text{Ry}^*$  corresponding to a 2D hydrogen atom.

Note that for the maximum concentration of impurities shown in Fig. 1,  $N^{2D} = 10^{14}/\text{cm}^2$ , the values obtained for the binding energies are still far from the strict 2D limit (4  $\text{Ry}^*$ ). We have checked, however, that for huge

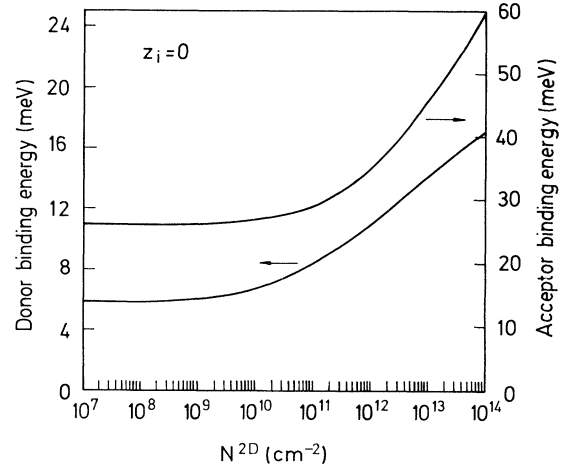


FIG. 1. On-center ( $z_i = 0$ ) donor (left scale) and acceptor (right scale) binding energies as functions of impurity concentration  $N^{2D}$ .

(unphysical) impurity concentrations the curves of Fig. 1 approach asymptotically their respective 2D limits.

From the results shown in Fig. 1 it is clear also that the donor impurity approaches the 2D limit faster than the acceptor impurity: for example, if  $N^{2D} = 10^{14}/\text{cm}^2$ , the ratio  $E(N^{2D}, 0)/(4 \text{ Ry}^*)$  takes the values of 0.71 and 0.58 for donors and acceptors, respectively. This has to do with the fact that because  $m_e^* < m_h^*$ , the wave function of the electron is more extended in the  $z$  direction (for the same electric field) and consequently feels the narrowing of the triangular well more intensely than the wave function of the hole.

We display in Figs. 2 and 3 the donor and acceptor binding energies, respectively, this time versus the impurity position  $z_i$ , for three different values of  $N^{2D}$ .

As expected on physical grounds, the binding energies

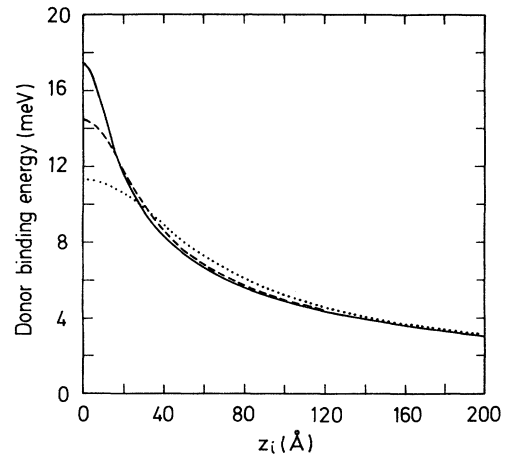


FIG. 2. Donor binding energy vs impurity position  $z_i$  for three values of impurity concentration: —,  $N^{2D} = 1.25 \times 10^{14}/\text{cm}^2$ ; ---,  $N^{2D} = 1.25 \times 10^{13}/\text{cm}^2$ ; ····,  $N^{2D} = 1.25 \times 10^{12}/\text{cm}^2$ .

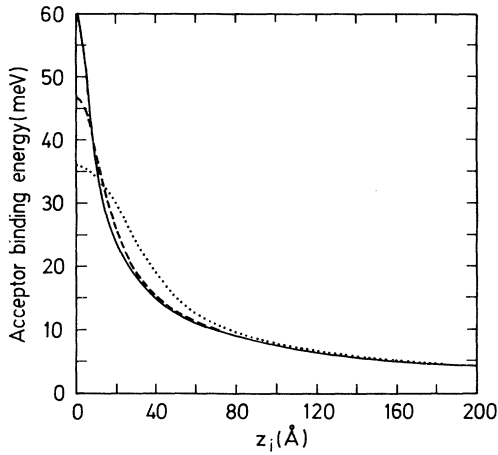


FIG. 3. Acceptor binding energy vs impurity position  $z_i$  for the same three values of  $N^{2D}$  as in Fig. 2.

are monotonic decreasing functions of  $z_i$ , going from a maximum value for  $z_i=0$  to very small values for  $|z_i| \gg \langle z^2 \rangle^{1/2}$  (see below). This is a consequence of the decreasing weight of the electron (or hole) wave function at the impurity position for increasing values of  $z_i$ .

When  $z_i=0$ , the maximum binding energy corresponds obviously to the greater  $N^{2D}$  (solid line in Figs. 2 and 3). However, when for a given impurity concentration  $z_i$  is larger than the corresponding impurity extension in the  $z$  direction (roughly given by  $\langle z^2 \rangle^{1/2}$ ) we expect larger binding energies for decreasing values of  $N^{2D}$ . This explains the crossover among the three curves observed in both figures.

As a consequence of the more localized character of the hole wave function ( $m_e^* < m_h^*$ ), the crossover is found for smaller values of  $z_i$  in the acceptor case (Fig. 3). We will return back to this point in our discussion of the vertical and lateral impurity extensions given below.

Finally, we present in Figs. 4 and 5 the lateral ( $\langle \rho \rangle$ ) and vertical ( $\langle z^2 \rangle^{1/2}$ ) extensions for the donor and acceptor impurities, respectively. In both figures  $z_i=0$ .

The dashed line [ $(\langle z^2 \rangle_0)^{1/2}$ ] corresponds to the mean value of the vertical extension, calculated with the exact solutions of  $H_0[f(z)]$ . The result is given by a closed analytical expression

$$(\langle z^2 \rangle_0)^{1/2} = \sqrt{A} \frac{|a'_1|}{(4\pi a_0^* N^{2D})^{1/3}} a_0^*, \quad (18)$$

where  $A$  is a constant defined by

$$A = \frac{8}{15} \left[ 1 + \frac{3}{8|a'_1|^3} \right].$$

In the 3D limit of low impurity concentrations, the lateral and vertical extensions  $\langle \rho \rangle$  and  $\langle z^2 \rangle^{1/2}$  approach asymptotically the above-mentioned 3D limits  $3\pi a_0^*/8$  and  $a_0^*$ , respectively. In the 2D limit of high-impurity concentrations, the lateral extension should approach the value  $a_0^*/2$  [Eq. (16)], while the vertical extension should

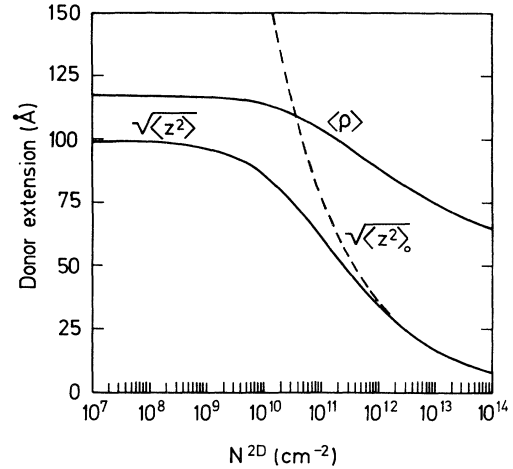


FIG. 4. Lateral ( $\langle \rho \rangle$ ) and vertical ( $\langle z^2 \rangle^{1/2}$ ) donor extension as functions of donor concentration;  $z_i=0$ . Dashed line: vertical extension calculated with the exact solutions of  $H_0$  [Eq. (18)].

go to zero, as a consequence of the narrowing of the triangular well. The results shown in Figs. 4 and 5 correspond to a smooth crossover between both limits.

The comparison between  $\langle z^2 \rangle^{1/2}$  and  $(\langle z^2 \rangle_0)^{1/2}$  shows nicely the complementary role played by  $f(z)$  and the exponential term in the trial wave function [Eq. (5)]. In the 3D limit, the exponential term is essential to give the correct physics (note that  $(\langle z^2 \rangle_0)^{1/2}$  diverges in this limit), while in the 2D limit, the confinement in the  $z$  direction is progressively given by the functions  $f(z)$  alone.

Note that in the donor case, for the highest impurity concentration  $N^{2D}=10^{14}/\text{cm}^2$ , the lateral extension  $\langle \rho \rangle \approx 65 \text{ Å}$ , still away from the 2D limit  $a_0^*/2 \approx 50 \text{ Å}$ ; this indicates again that for this value of  $N^{2D}$  the donor impurity is not in the complete 2D regime.

The same conclusion holds for the acceptor case, with

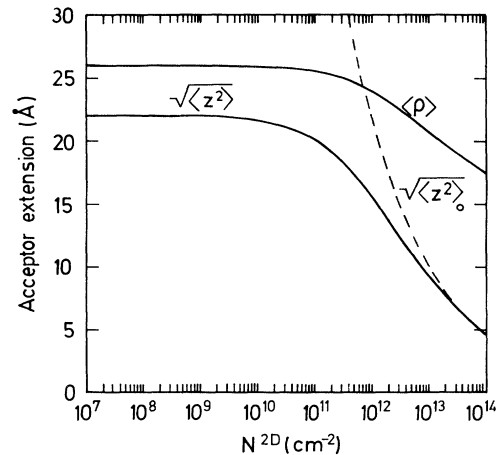


FIG. 5. Lateral ( $\langle \rho \rangle$ ) and vertical ( $\langle z^2 \rangle^{1/2}$ ) acceptor extension as functions of acceptor concentration;  $z_i=0$ . Dashed line: vertical extension calculated with the exact solutions of  $H_0$  [Eq. (18)].

the difference that, as explained above, the 2D limit is reached more slowly than in the donor case. For example, for  $N^{2D} = 10^{14}/\text{cm}^2$ ,  $\langle \rho \rangle / (a_0^* / 2)$  takes the values 1.3 and 1.6 for donors and acceptors, respectively. (In the complete 2D limit, the ratio must be 1).

As mentioned above, the fact that the crossover found among the different curves in Figs. 2 and 3 occurs for smaller values of  $z_i$  for acceptors than for donors, can be explained with the results of Figs. 4 and 5. As can be seen from these figures, for any value of  $N^{2D}$ ,  $(\langle z^2 \rangle^{1/2})_{\text{electrons}} \gg (\langle z^2 \rangle^{1/2})_{\text{holes}}$ , and consequently, the condition  $z_i \simeq (\langle z^2 \rangle^{1/2})$  and the corresponding crossover is fulfilled earlier for the acceptors.

In summary, we have calculated, within the effective-mass approximation, the ground-state binding energy and spatial extension of donor and acceptor shallow impurities in triangular GaAs quantum wells. While the main part of the discussion has been focused on the case of  $\delta$ -doped  $n$ - $i$ - $p$ - $i$  structures, our results are equally applicable to the problem of shallow impurities in compositionally graded superlattices.

The binding energy of on-center hydrogenic impurities in triangular GaAs quantum wells increases monotonically from the 3D limit (low-impurity concentrations) to the 2D limit (high-impurity concentrations). This is in contrast with the behavior of shallow impurities in GaAs-Ga<sub>1-x</sub>Al<sub>x</sub>As quantum wells, where at the zero thickness well limit, in the realistic case of a finite barrier, the electron (hole) wave function is entirely in Ga<sub>1-x</sub>Al<sub>x</sub>As and one recovers the bulk (3D) value of the binding energy of the donor (acceptor) in this material.

For a typical value of the triangular potential ( $N^{2D} \simeq 10^{13}/\text{cm}^2$ ) while the lateral extension of the impurity is given by the Coulombic attraction between carrier and impurity, the vertical extension is essentially given by the confinement effect of the triangular potential.

We believe that the results presented in this work may be useful in the qualitative understanding of future experimental work on shallow impurities in sawtooth-doped superlattices.

\*Permanent address: Instituto de Física de Ciencias Exactas y Tecnología, Universidad Nacional de Tucumán, Avenida Roca 1800, 4000 San Miguel de Tucumán, Argentina.

<sup>1</sup>See, for example, *Molecular Beam Epitaxy and Heterostructures*, edited by L. L. Chang and K. Ploog (Nijhoff, Dordrecht, 1985).

<sup>2</sup>L. Esaki, in *Proceedings of the 17th International Conference on the Physics of Semiconductors, San Francisco, 1984*, edited by J. D. Chadi and W. A. Harrison (Springer-Verlag, New York, 1985).

<sup>3</sup>L. Esaki, *IEEE J. Quantum Electron.* **QE-22**, 1611 (1986).

<sup>4</sup>B. V. Shanabrook and J. Comas, *Surf. Sci.* **142**, 504 (1984).

<sup>5</sup>B. V. Shanabrook, J. Comas, T. A. Perry, and R. Merlin, *Phys. Rev. B* **29**, 7096 (1984).

<sup>6</sup>N. C. Jarosik, B. D. McCombe, B. V. Shanabrook, J. Comas, J. Ralston, and G. Wicks, in *Proceedings of the 17th International Conference on the Physics of Semiconductors* (Ref. 2).

<sup>7</sup>R. C. Miller, A. C. Gossard, W. T. Tsang, and O. Munteanu, *Phys. Rev. B* **25**, 3871 (1982).

<sup>8</sup>R. L. Greene and K. K. Bajaj, *Solid State Commun.* **53**, 1103 (1985).

<sup>9</sup>G. Bastard, *J. Lumin.* **30**, 488 (1985).

<sup>10</sup>C. Delalande, *Physica* **146B**, 112 (1987).

<sup>11</sup>B. V. Shanabrook, *Physica* **146B**, 121 (1987).

<sup>12</sup>Y.-C. Chang, *Physica* **146B**, 137 (1987).

<sup>13</sup>E. F. Schubert, B. Ullrich, T. D. Harris, and J. E. Cunningham,

*Phys. Rev. B* **38**, 8305 (1988).

<sup>14</sup>B. Ullrich, C. Zhang, E. F. Schubert, J. E. Cunningham, and K. v. Klitzing, *Phys. Rev. B* **39**, 3776 (1989).

<sup>15</sup>E. F. Schubert, T. D. Harris, J. E. Cunningham, and W. Jan, *Phys. Rev. B* **39**, 11011 (1989).

<sup>16</sup>E. Ullrich, C. Zhang, and K. v. Klitzing, *Appl. Phys. Lett.* **54**, 1133 (1989).

<sup>17</sup>K. Ploog and G. H. Döhler, *Adv. Phys.* **32**, 285 (1983).

<sup>18</sup>C. R. Proetto, *Phys. Rev. B* **41**, 6036 (1990).

<sup>19</sup>G. H. Döhler, *Phys. Status Solidi B* **52**, 79 (1972).

<sup>20</sup>J. M. Ferreyra and C. R. Proetto, *Phys. Rev. B* **42**, 5657 (1990).

<sup>21</sup>P. Ruden and G. H. Döhler, *Phys. Rev. B* **27**, 3538 (1983).

<sup>22</sup>G. H. Döhler, in *Properties of Impurity States in Superlattice Semiconductors*, edited by C. Y. Fong, I. P. Batra, and S. Ciraci (Plenum, New York, 1988), p. 159.

<sup>23</sup>E. F. Schubert, T. D. Harris, and J. E. Cunningham, *Appl. Phys. Lett.* **53**, 2208 (1988).

<sup>24</sup>E. F. Schubert (private communication).

<sup>25</sup>F. Capasso, S. Luryi, W. T. Tsang, C. G. Bethea, and B. F. Levine, *Phys. Rev. Lett.* **51**, 2318 (1983); F. Capasso, *Annu. Rev. Mater. Sci.* **16**, 263 (1986).

<sup>26</sup>*Handbook of Mathematical Functions*, edited by M. Abramowitz and I. A. Stegun (Dover, New York, 1970), p. 446.

<sup>27</sup>L. E. Oliveira and L. M. Falicov, *Phys. Rev. B* **34**, 8676 (1986).